Synthesis and Characterization of Polyaniline–Organoclay Nanocomposites

N. Salahuddin, M. M. Ayad, M. Ali

Department of Chemistry, Faculty of Science, Tanta University, 31527 Tanta, Egypt

Received 30 January 2007; accepted 10 August 2007
DOI 10.1002/app.27180
Published online 30 October 2007 in Wiley InterScience (www.interscience.wiley.com).

ABSTRACT: Polyaniline (PANI)–organoclay nanocomposites were prepared. Intercalation of aniline monomer into montmorillonite (MMT) modified by polyoxyalkylene was followed by subsequent oxidative polymerization of the aniline in the interlayer spacing. The organoclay was prepared by cation exchange process between sodium cation in MMT and onium ion in four different types of polyoxyalkylene diamine and triamine with different molecular weight. Infrared spectra confirm the electrostatic interaction between the positively charged onium group (NH_3^+) and the negatively charged surface of MMT. X-ray diffraction analysis provides a structural information. The absence of d_{001} diffraction band in the nanocomposites was observed at certain types and contents of organoclay. Scanning electron microscopy and transmission electron microscopy were employed to determine the dispersion of the clay into PANI. The thermal degradation behavior of PANI in the nanocomposites has been investigated by thermogravimetric analysis. The weight loss suggests that the PANI chains in the nanocomposites are more thermally stable than pristine PANI. This improvement is attributed to the presence of nanolayers with high aspect ratio acting as barriers, thus shielding the diffusion of degraded PANI from the nanocomposites. The electrical conductivity of the nanocomposites was increased 30 times more than that of pure MMT at a certain concentration. © 2007 Wiley Periodicals, Inc. J Appl Polym Sci 107: 1981–1989, 2008

Key words: nanocomposites; polyaniline; organoclay

INTRODUCTION

Polyaniline (PANI) is one of the most technologically important materials because of its environmental stability in conducting form, low cost of synthesis, and high conductivity. These properties provide possible applications in battery electrodes,[1,2] electrochromic devices,[3,4] energy storage devices,[5] and photoelectric cell.[6] However, the major problems related to its successful utilization lie in its poor mechanical properties and processability, and its insoluble nature in common organic solvents makes PANI unsatisfactory for practical applications. Many attempts have been made to improve these aspects by blending the PANI with thermoplastics[7–10] and thermosetting polymers.[11]

Interaction between layered silicate materials and polymers has attracted interests. Dispersion of layered silicate in the polymers has resulted in enhancements of mechanical and thermal properties of the matrix at unexpectedly small inorganic contents.[12,13] Layered silicate–polymer nanocomposites have been prepared using an incredibly wide range of polymers including polystyrene,[14] polymethylmethacrylate,[15] butadiene acrylonitrile copolymer,[16,17] epoxy,[18,19] polyoxyethylene methacrylate,[20] and nylon.[21] Four general methods have been reported for preparing PANI-clay nanocomposites.[22–26] The first one consists of the use of transition metal ions (Cu^{2+}) introduced as exchangeable cations into homoionic smectite to induce direct topotactic PANI formation.[27] The second procedure is based on the previous exchange of the interlayer cations (Na^+) by anilinium species, which are subsequently polymerized by means of an oxidizing agent such as ammonium peroxodisulphate.[28] The third method involves the addition of PANI to the reaction media in which the clay is hydrothermally synthesized.[29] Finally, the fourth method is emulsion polymerization, in which the emulsifier in emulsion system contributes to maximization of the affinity between hydrophilic host (clay) and hydrophobic guest (aniline).[30]

The goal of this work is to investigate the *in situ* aniline polymerization reaction between the layers of modified montmorillonite (MMT). In our work, MMT exchanged with polyoxyalkylene intercalate aniline and then ammonium peroxydisulphate (APS) was added subsequently as oxidizing agent to initiate polymerization of aniline between the layers. The characterization of PANI-MMT nanocomposites was performed by X-ray diffraction (XRD), scanning electron microscopy (SEM), and transmission electron

Correspondence to: N. Salahuddin (nasgad@yahoo.com).

Journal of Applied Polymer Science, Vol. 107, 1981–1989 (2008)

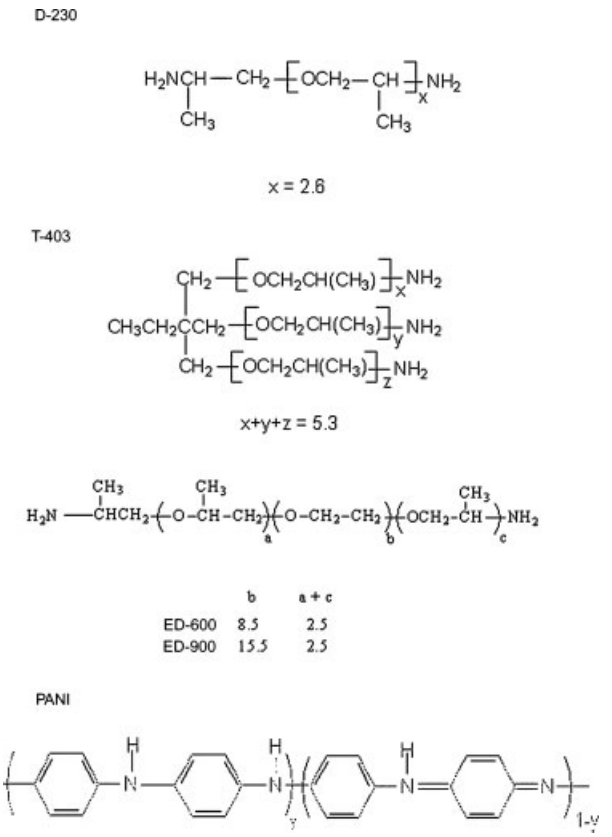

Figure 1 General structure of PANI, Jeffamine D-230, Jeffamine T-403, Jeffamine ED-600, and Jeffamine ED-900.

microscopy. In addition, the thermal and electrical conductivity of the nanocomposites were measured.

EXPERIMENTAL

Chemicals

The clay used in this study was MMT from Southern Clay Products Inc. (Gonzales, TX) under the trade name of mineral colloid BP. The MMT was received as fine particles. The reported cation exchange capacity was 114.8 meq/100 g. The d_{001} (interlamellar or interlayer) spacing measured at ambient humidity is 12 and 9.6 Å after drying in a vacuum oven at 100°C for 12 h. Polyoxypropylene diamine, Jeffamine D_{230}, (D_{230}) has an average molecular weight of 230, Brookfield viscosity at 25°C is 9 and the primary amine content is 8.3 meq/g; polyoxypropylenetriamine, Jeffamine T_{403}, (T_{403}) has an average molecular weight of ~ 440, Brookfield viscosity at 25°C is 70 and the primary amine content is 6.1 meq/g; polyoxyethylenediamine, which are aliphatic primary diamines structurally derived from propylene oxide-capped polyethylene glycol, under the trade name of Jeffamine ED_{600} (ED_{600}) has an average molecular weights 600 and the amine content is 3.19 meq/g; Jeffamine ED_{900} (ED_{900}) has an average molecular weight of 900, and the amine content is 2.05 meq/g were obtained from Huntsman Corporation. The chemical structure of Jeffamines is shown in Figure 1. Aniline was purified by vacuum distillation. Ammonium peroxydisulphate (APS; B.D.H.) was used as received. Both aniline and APS were stored at 4°C.

Preparation of organoclay nanocomposites

The organoclay was prepared by a cation-exchange reaction between the sodium cations of MMT and NH_3^+ groups in Jeffamines. Typically, 10 g of MMT was suspended in 300 mL distilled water and stirred for 3 h at 60°C followed by stirring overnight at room temperature. An aqueous solution of 2.8 g of acidified D_{230} with HCl aqueous solution was added to the swelled clay with constant stirring. The mixture was then stirred for an additional 24 h. The precipitate was filtered and washed with water several times, until no chloride ions were detected in the filtrate by testing with $AgNO_3$. The resultant product (I) was dried at 60°C to give 7.134 g. The same procedure was followed for the other types of Jeffamines (Table I).

Preparation of PANI/organoclay nanocomposites

As a typical procedure for the preparation of the PANI/D_{230}-MMT nanocomposite materials, first 0.9 g of aniline was added to 0.0183 g of D_{230}-MMT (I) swelled in 5 mL DMF and stirred for 24 h at room temperature followed by stirring for 3 h at 60°C. The mixture was cooled to 0°C. APS (2.2 g) dissolved in 50 mL 0.1*M* HCl was added drop wise and the polymerization continued for 24 h. The molar ratio between aniline and APS was 1 and the concentration of aniline was 0.18*M*/L. The dark green precipitate (I_a) was washed with a large amount of 0.1*M* aqueous HCl solution several times and with methanol. The product was filtered and dried at 50°C. For the sake of comparison, different types and different contents (2–50 wt %) of organoclays have been used to prepare PANI/organoclay nanocomposites (Table II).

TABLE I
Composition and X-ray Data of Organoclay

	Jeffamine		MMT	Organoclay			
				Yield		X-ray data	
Code	Type	wt (g)	wt (g)	wt (g)	wt %	2θ	*d*-spacing (Å)
I	D_{230}	2.8	10	7.13	55.7	6.3	14.0
II	T_{403}	3.7	10	8.00	58.4	6.0	14.7
III	ED_{600}	7.1	10	8.82	57.4	5.1	17.3
IV	ED_{900}	11	10	10.44	49.7	5.0	17.6

TABLE II
Composition Data of Organoclay/PANI Nanocomposites

Code	Organoclay		
	Type	wt (g)	wt (%)
I_a	D_{230}-MMT	0.0183	2
I_b	D_{230}-MMT	0.146	14
I_c	D_{230}-MMT	0.300	25
I_d	D_{230}-MMT	0.900	50
II_a	T_{403}-MMT	0.0183	2
II_b	T_{403}-MMT	0.146	14
II_c	T_{403}-MMT	0.300	25
II_d	T_{403}-MMT	0.900	50
III_a	ED_{600}-MMT	0.0183	2
III_b	ED_{600}-MMT	0.146	14
III_c	ED_{600}-MMT	0.300	25
III_d	ED_{600}-MMT	0.900	50
IV_a	ED_{900}-MMT	0.0183	2
IV_b	ED_{900}-MMT	0.146	14
IV_c	ED_{900}-MMT	0.300	25
IV_d	ED_{900}-MMT	0.900	50

The molar ratio between aniline and APS was 1 and the concentration of aniline was 0.18*M*/L.

Characterization

XRD data on the powdered samples were determined by an autodiffractometer, which consists of a Phillips XRG 3100 X-ray generator equipped with a Ni-filtered Cu Kα (λ = 1.5418 Å) X-ray source connected to a Phillips APD 3520 type PW 1710 diffractometer controller. The scanning speed was 0.005°/s. The samples were dried in a vacuum oven at 80°C for 12 h, then mounted on a sample holder with a large cavity, and a smooth surface was obtained by pressing the samples with a glass plate. Bragg's law ($n\lambda = 2d \sin\theta$) was used to compute the crystallographic spacing. Infrared absorption spectra were carried out on a Perkin–Elmer 1420 spectrophotometer, using KBr disc technique in the wavelength range of 4000–600 cm^{-1}. Thermogravimetric analysis (TGA) was carried using Perkin–Elmer thermal analyzer system at a heating rate of 10°C/min from 30 to 800°C under nitrogen atmosphere. A JEOL JSM 5400 SEM was used to observe the particle size of MMT and the particle matrix adhesion in the composite on the fractured surface. The pellets of samples used for morphology examination were prepared by pressing the powders. The pressed specimens were then fractured and the fracture surface was sputtered with gold prior to observation. The morphologies of the nanocomposites with different PANI content at 20 kV of accelerating voltage were also measured. Transmission electron microscopy (TEM) specimens were cut from nanocomposite block using an ultramicrotome, LKB 8800 ultramicrotome III equipped with a glass knife. The ground fine powders were dispersed in a low viscosity epoxy resin. After curing, the ultrathin films were cut by moving the sample across a knife edge of glass. The ultrathin flakes floats onto a trough filled with water, from where they were collected on 200-mesh copper grids and dried at room temperature. TEM micrographs were taken with a JEOL JEM-100CX electron microscope at an accelerating voltage of 100 kV. The intensity of electron beam should be minimized in order to prevent degradation of the samples. A Simpson 260 VOM multimeter and a Keithley 617 electrometer were used to measure the conductivity at room temperature for the samples two times, using the two-point probe technique, and the average values were taken.

RESULTS AND DISCUSSION

The general structure of PANI can be expressed as shown in Figure 1. Different forms of PANI according to *y*-value. The conductive form of PANI is the protonated emeraldine or emeraldine salt (ES) whose color is green and the conductivity is around15 S/cm,[15] whereas the conductivity of emeraldine base (EB) is around 10^{-5} S/cm.

On the other hand, MMT is a clay mineral and belongs to the general family of 2 : 1 layered silicate. Their structure consists of two fused silica tetrahedral sheets sandwiching an edge-shared octahedral sheet of either magnesium or aluminum hydroxide. Stacking of the layers leads to a regular van der Waals gap or interlayer. Isomorphic substitution within the layers generates negative charges that are counterbalanced by Na^+ or Ca^{2+} cations residing in the interlayers. These cations can be replaced by organic cations (alkylammonium ions) by a cationic-exchange reaction to render the hydrophilic layered silicate organophilic. MMT has a high swelling capacity, which is important for efficient intercalation of the polymer, and is composed of stacked silicate sheets that offer enhanced thermal stability, mechanical strength, fire-retardant and barrier properties.

The synthetic procedure used for nanocomposite preparation is essentially developed by Usuki et al. for nylon–silicate nanocomposite.[21] It involves dispersion of the organically modified clay in a suitable monomer followed by polymerization. A similar synthetic protocol in the present study was used in the preparation of PANI-MMT nanocomposites. This involved mixing of clay modified by Jeffamines with aniline monomer in the presence of suitable solvent followed by addition of oxidizing agent to initiate polymerization between the layers. Under proper conditions, exfoliation of the organoclay into individual silicate layers occurs, which ultimately becomes dispersed within the macromolecular matrix.

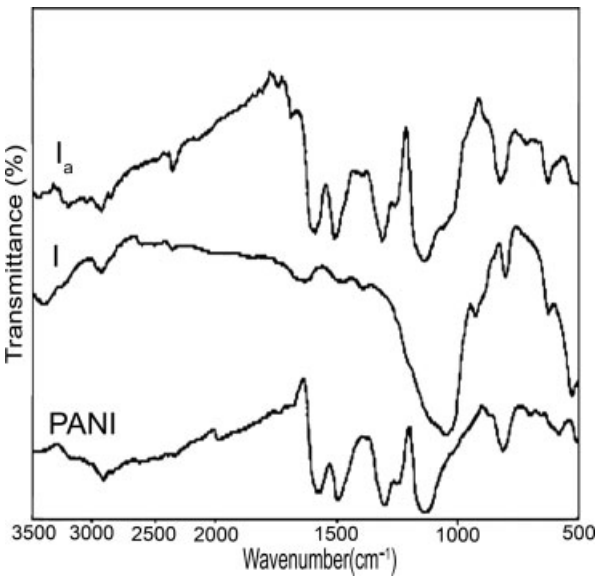

Figure 2 IR spectra of PANI, D_{230}-MMT (I), and PANI/D_{230}-MMT nanocomposites (I_a) in the region of 4000–700 cm^{-1}.

Figure 2 shows IR spectra of organoclay D_{230}-MMT (I), pure PANI, and PANI/D_{230}-MMT (I_a) nanocomposite. Characteristic bands corresponding to MMT in organoclay are shown at 1044 cm^{-1} (ν(Si—O)), 919 cm^{-1} (δ(Al—OH)) and 520 cm^{-1} (ν(Si—O—Al)). The band at 1461 cm^{-1} can be assigned to stretching (C—N), while bands at 3423 cm^{-1}, 1632 cm^{-1} can be attributed to the N—H stretching and bending modes of the NH_3^+ group,[31,32] confirming the presence of ionic bond between D_{230} and MMT.

The characteristic vibration bands for PANI are shown in Figure 2. The broad band at 3441 cm^{-1} is due to the characteristic free N—H stretching vibration, which suggests the presence of secondary amino groups (—NH—). The weak band at 2921 cm^{-1} arises from the aromatic C—H stretching vibration. The characteristic band appearing at 1477 cm^{-1} corresponds to the benzenoid ring stretching frequency and the peak appearing at 1579 cm^{-1} corresponds to the quinoid ring stretching frequency. The absorption band at 1293 cm^{-1} is due to C—N stretching vibration of secondary aromatic amine. The band characteristic of the conducting protonated form is observed at 1238 cm^{-1}. It has been interpreted as $C—N^{+\bullet}$ stretching vibration in the polaron structure. The 1124 cm^{-1} band can be assigned to a vibration mode of the $—NH^+=$ structure, which is formed by protonation. The broad nature of this peak is due to the high degree of electron delocalization which was expected because of the greater degree of oxidation. The C—H out-of-plane bending vibration band of 1,4-disubstituted benzene ring appears at 796 cm^{-1}. These observed bands are in good agreement with previously published values.[33]

It was reported that there are physical interactions between the intercalated PANI and MMT.[25] As can be seen, the clay band dominates IR spectra at 1044 cm^{-1} in the composite, making the analysis of this spectral region difficult. IR spectra of the composite show characteristic bands of pure PANI indicating the existence of PANI in the ES form. Comparing the free PANI with PANI/D_{230}-MMT(I_a) nanocomposites, it is noticed that the characteristic band for C—N stretching in the free PANI has their counterpart band in the nanocomposites spectra, indicating that the same kind of polymerization occurs inside the gallery. However, it is worth noting from a closer look at the spectra that there is a shift of the band at 1293 cm^{-1} that assigned as stretching vibration of (ν(C—N)) to 1298 cm^{-1}. The frequency shift of (ν(C—N)) observed in this composite is due to physical interaction between PANI chain and silicate layers. In addition, the band at 1238 cm^{-1} in PANI that attributed to $C—N^{+\bullet}$ stretching vibration in the polaron structure shifts to 1247 cm^{-1} in PANI/D_{230}-MMT. This indicates that the electrostatic interaction between the positive charge of PANI and the negatively charged surface of the clay layers affects the vibrational motion of PANI.

XRD pattern of the clay modified by D_{230}, T_{403}, ED_{600}, and ED_{900} was shown in Figure 3(a–d). The organoclay powders showed a strong diffraction peak with a characteristic interlayer spacing of 14 and 14.7 Å for D_{230} and T_{403}, respectively, that was very close to the reported spacing.[19] Clay modified by ED_{600} and ED_{900} showed a sharp peak with a spacing of 17.3 Å and a broad peak with a spacing of 17.6 Å, respectively. Taking into account a layer thickness of 9.3 Å, the basal spacing of 14, 14.7, 17.3, and 17.6 Å corresponds to a gallery height of 4.7, 5.4, 8.0, and 8.3 Å, respectively. The peak appears at large angle ($2\theta = 20^\circ$) in all the diffraction patterns corresponds to the crystallographic plane (110) and (020) of the clay layers. The presence of this peak demonstrates that the XRD analysis is sensitive enough to detect the presence of the clay in the composites.[34]

The peak characteristic to D_{230}-MMT and T_{403}-MMT was disappeared in PANI/organoclay nanocomposites with different concentration of D_{230}-MMT and T_{403}-MMT. This indicates that almost complete exfoliation of the silicate layers takes place, and a nanocomposite structure was obtained. A notable small broad diffraction peak at $2\theta = 4.2^\circ$(20.5 Å) was appeared. This peak was observed in pure PANI. However, in PANI/organoclay nanocomposites using ED_{600}, it was noted that intense XRD signals from organoclay peaks are apparent in nanocomposites containing 50 wt % organoclay. When

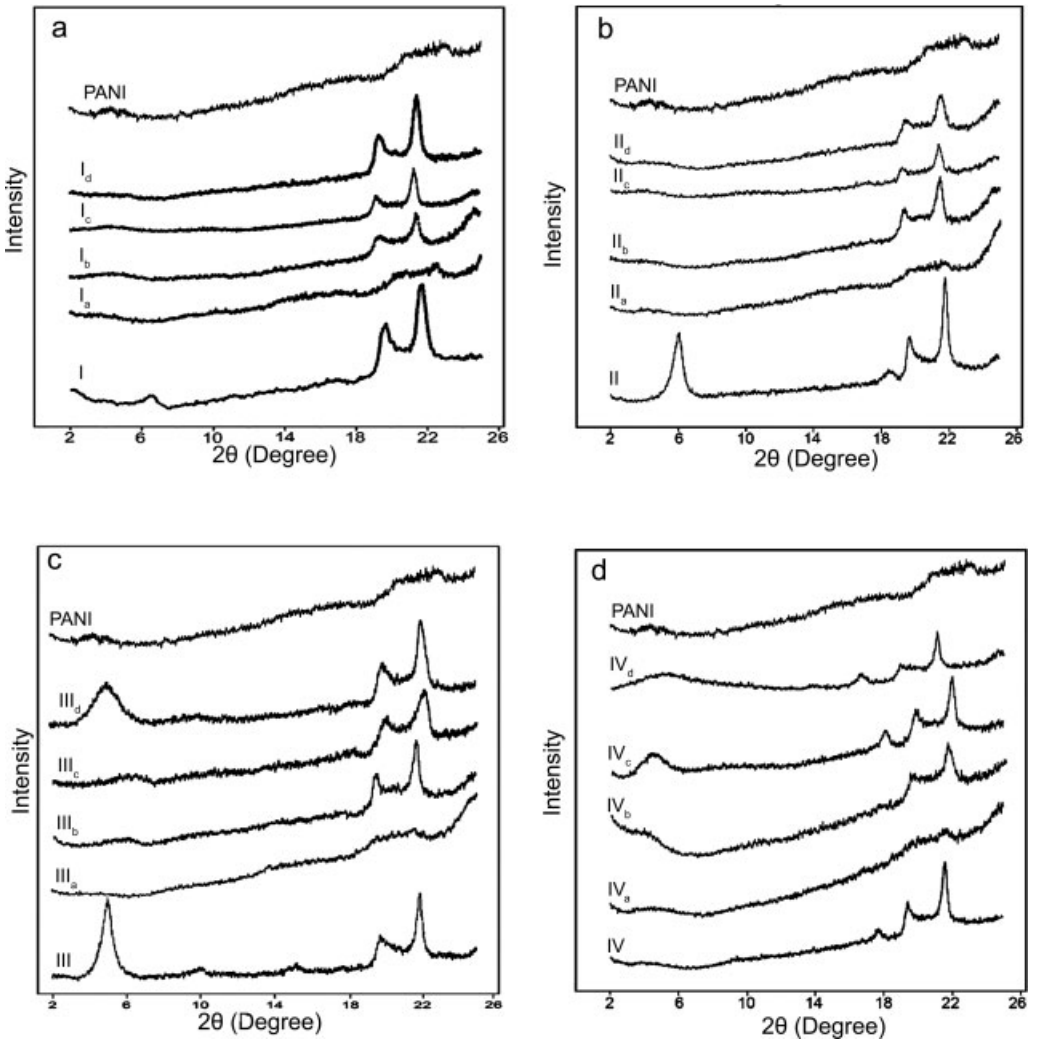

Figure 3 X-ray diffraction pattern of (a) PANI, D_{230}-MMT, and PANI/D_{230}-MMT nanocomposites; (b) PANI, T_{403}-MMT, and PANI/T_{403}-MMT nanocomposites; (c) PANI, ED_{600}-MMT, and PANI/ED_{600}-MMT nanocomposites; (d) PANI, ED_{900}-MMT, and PANI/ED_{900}-MMT nanocomposites at different organoclay concentrations.

the amount of organoclay decreases (25 and 14 wt %), the peak characteristic to the organoclay disappeared and broad peaks appeared at 2θ equals 6°. If the nanocomposite contains 2 wt % of organoclay, the peak disappeared. The intercalation of more polymer chain inside clay layers lead to disordering of the layered clay structure. Similar behavior was obtained for PANI/organoclay using ED_{900}, Figure 3(d), except that the broad peaks of the organoclay were slightly shifted to lower 2θ. The inefficient exfoliation of MMT in these two systems at high concentration was related to the swelling properties of organoclay in DMF. ED_{600}-MMT was much less swollen by DMF than does ED_{900}. This indicates that the type and the molecular weight of the polyoxyalkylene used in modification of the clay affects the morphology of the resulting material. It is worth mentioning that many studies on PANI/clay nanocomposites have been carried out, and an intercalated structure was obtained.[35,36] The basal spacing of PANI-smectite clay nanocomposites was varied from 13 to 15 Å depending on the experimental conditions in the polymerization of aniline species. It was assumed that the rings in a pseudoplanar or tilted arrangement with respect to the (a,b) silicate plane. However, Porter[36] has claimed the possible formation of mono- and bilayers of PANI in the interlayer regions of clays.

It was reported that the elementary building block of the composite may erect an aggregate of a microscale[37] or a nanostructure[16]. To more clearly identify the structure of the nanocomposites, TEM images of the PANI/D_{230}-MMT at different concentrations were shown in Figure 4. Dark stripes represent the clay layers and the gray/white area represents the polymer matrix[24]. At low concentration [Fig. 4(a)], TEM images show nanosized clay domains with an average size of 150 nm. On the other hand, the TEM

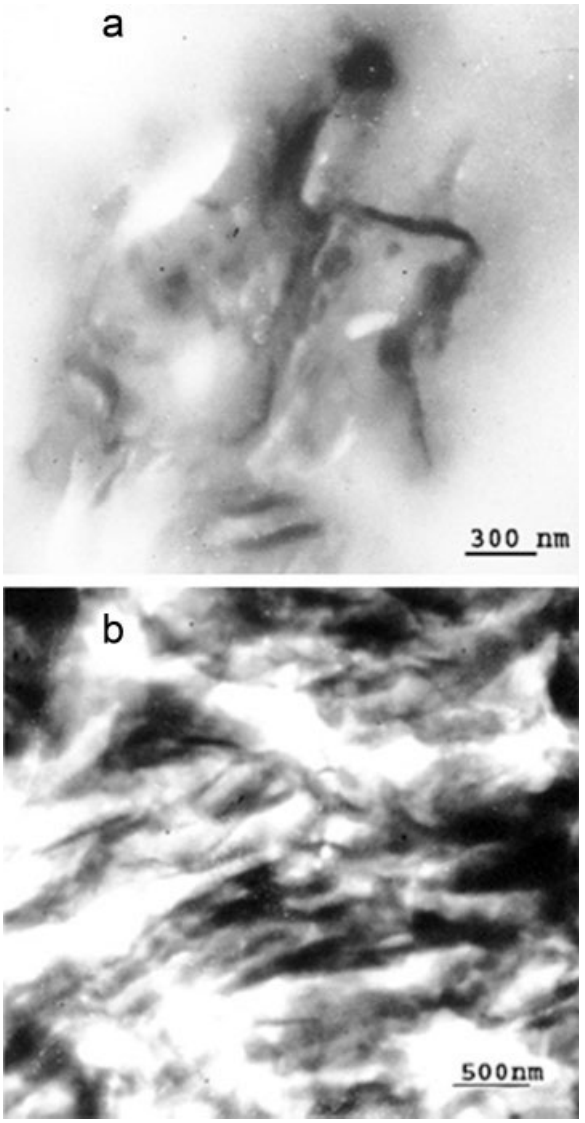

Figure 4 TEM images of PANI/D_{230}-MMT nanocomposites using (a) 2 wt % of D_{230}-MMT; (b) 50 wt % of D_{230}-MMT.

of the composites at a high concentration of organoclay [Fig. 4(b)] has a considerable amount of stacked layers with an average size of 250 nm in which polymer chains are intercalated as evidenced from XRD.

SEM images of PANI and PANI/organoclay nanocomposites are shown in Figure 5. The microstructure of PANI particles was compared with that of the composites. It can be seen that the PANI particles [Fig. 5(a)] have a spherical shape with porous structure. The average diameter of PANI is 200 nm. In case of PANI/D_{230}-MMT nanocomposites [Fig. 5(b,c)], it is worth noting that examination of the fractured surface did not reveal inorganic aggregation, indicating that the mineral domains are homogenously dispersed in the polymer matrix. At high magnification, both plate-like structure and spherical particles are shown. It can be easily assumed that spherical particles are pure PANI. The plate-type particles represent a hybrid of PANI and clay particles, which was formed during the polymerization step. The spheroidal morphology typical of the neat PANI is hardly observable in the presence of high D_{230}-MMT content, and plate-like particles are

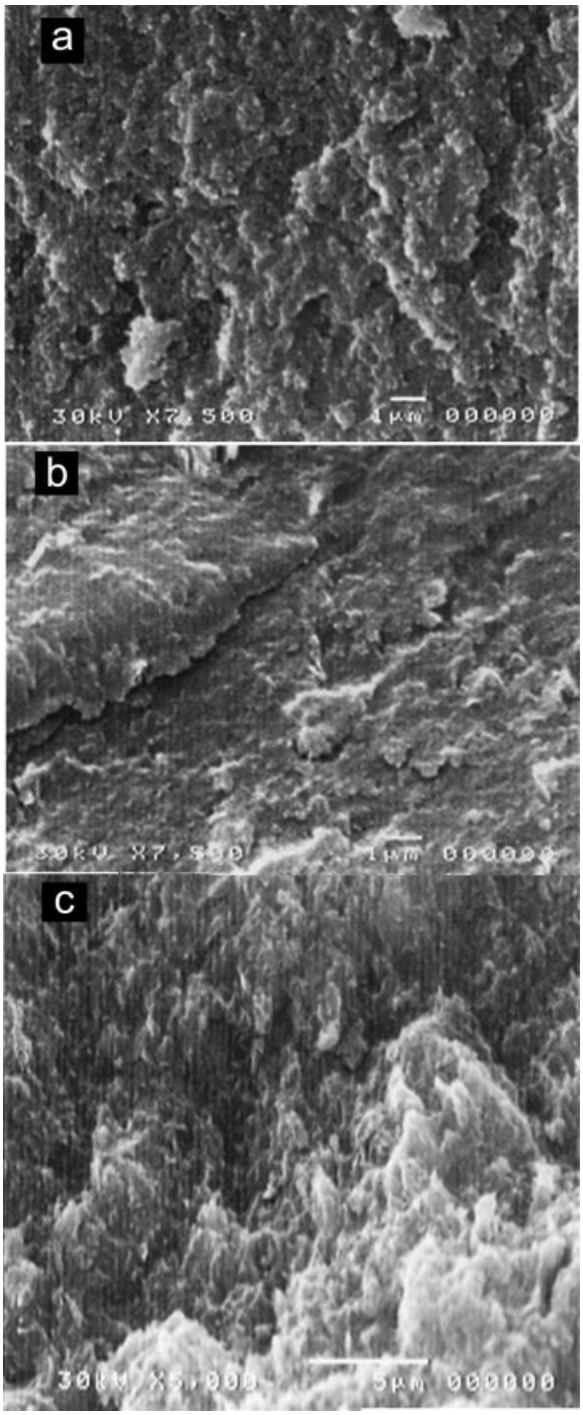

Figure 5 Scanning electron micrograph of (a) PANI, (b) PANI/D_{230}-MMT at 2 wt % of D_{230}-MMT, (c) PANI/D_{230}-MMT at 50 wt % of D_{230}-MMT.

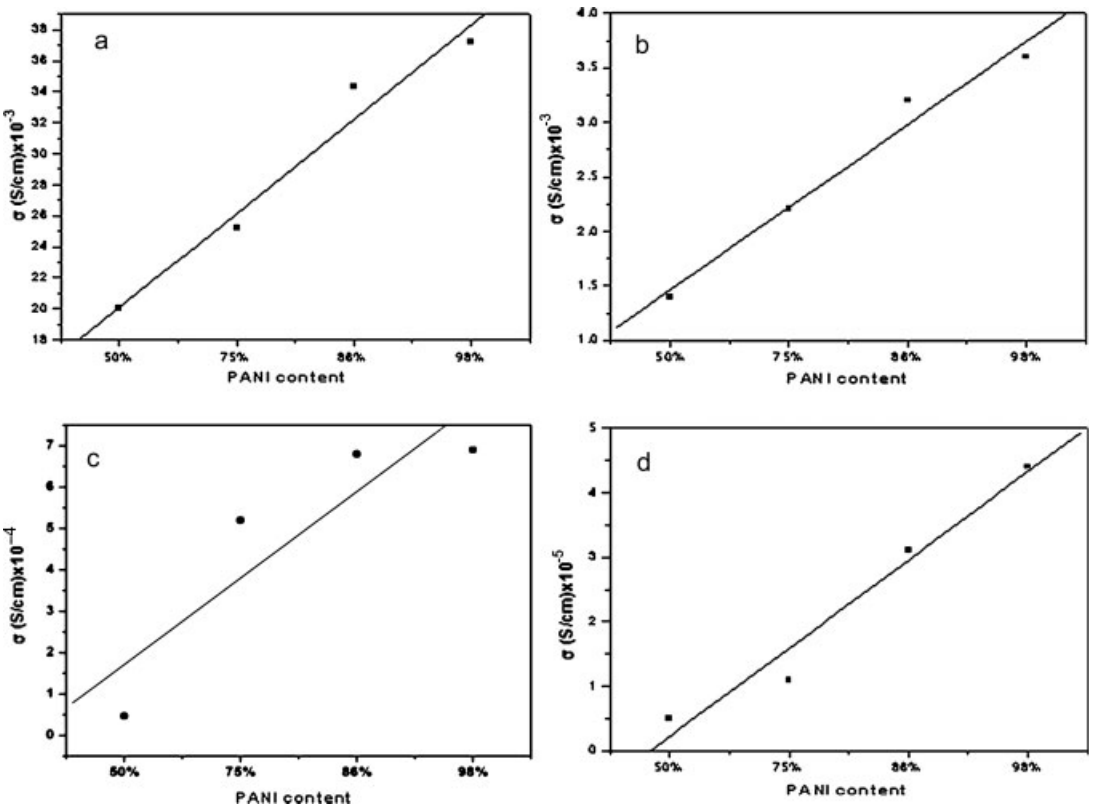

Figure 6 Electrical conductivity of PANI/organoclay nanocomposites at different concentrations of PANI using (a) D_{230}-MMT, (b) T_{403}-MMT, (c) ED_{600}-MMT, and (d) ED_{900}-MMT.

noticed. It should also be noted that most of the PANI chains are intercalated into the interlayer spacing of MMT as shown in XRD data. However, in case of 2 wt % of D_{230}-MMT, it can be clearly seen free of PANI particles.

The room temperature conductivity (σ_{RT}) of PANI/organoclay nanocomposites varies from 5×10^{-6} to 3.72×10^{-2} S/cm. There exists an increase in s_{RT} in PANI composites with increasing PANI content, as shown in Figure 6. The presence of high content of free PANI chains facilitate the electron transfer between the intercalated PANI chains, presumably because of the connectivity of free PANI chains. It is worth noting that the conductivity of nanocomposites at a certain concentration of organoclay decreases with increasing molecular weight of Jeffamine. The chain length may preclude interchain interaction and decrease the conductivity of the system. It was reported[13,24] that the conductivity of electroactive polymer–clay nanocomposites is always lower than that of the corresponding parent guest polymer without clay. These composites result from the assembly of a conducting polymer separated by individual silicate layers of insulating character. Moreover, electrical transport through short and narrow intercalated polymer chains is strongly disfavored. The constrained polymer in the intracrystalline region can impose chain conformation changes that also contribute to a decrease in the conductivity of the system.

Mehrota and Giannelis[38] carried out the intercalative polymerization of aniline using a Cu^{2+}-exchanged synthetic clay (hectorite). The electronic absorption spectrum of the resulting nanocomposites showed the characteristic insulating PANI form (EB). To obtain the conducting material, it was necessary to dope the nanocomposite by exposure to HCl vapors. As a consequence of this treatment, PANI ES was formed in the interlayer region. It was reported that the conductivity of PANI-clay materials prepared from anilinium MMT is 10^{-6} S/cm,[35] which is lower than that of the corresponding nanocomposites obtained as described by Mehrota and Giannelis[38] (5×10^{-2} S/cm). Such discrepancy was ascribed to the high anisotropy behavior conductivity in this type of material. Besides, the nature of the PANI chains (length, oxidation, and protonation extent) may also be different from one system to another, thereby affecting their conductivity. It should also be taken into account that the maximum conductivity of PANI-clays depends on aggregation states of PANI chains and that, for the intercalated materials containing isolated molecular wires, the conductivity is lower than that in the bulk PANI.

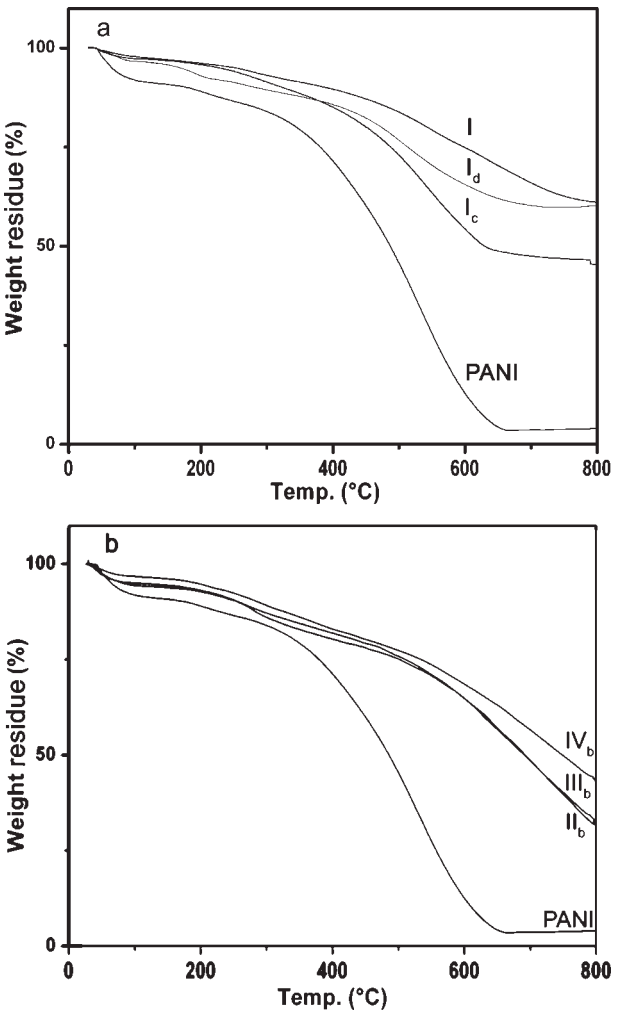

Figure 7 (a) TGA curves of PANI, D_{230}-MMT (I), PANI/D_{230}-MMT nanocomposites containing 25 wt % (I_c), 50 wt % (I_d) of D_{230}-MMT; (b) PANI/organoclay nanocomposites at 14 wt % of T_{403}-MMT (II_b), ED_{600}-MMT (III_b), ED_{900}-MMT (IV_b).

Figure 7(a) depicts TGA thermograms of the D_{230}-MMT, PANI, and PANI/D_{230}-MMT nanocomposites. There are four major stages of weight loss for the organically modified clay (D_{230}-MMT). The first weight loss below 100°C is a result of the release of free water. The second and third stages in the temperature range of 200–600°C are associated with the decomposition of the intercalated polyoxypropylene in the organoclay. The lower molecular weight is released first at lower temperature, followed by the higher molecular weight. In the last stage of weight loss in the temperature range of 600–780°C, the structural water that is bonded to hydroxyl groups start to decompose and is being released. For pure PANI, a small weight loss around 100°C is presumably due to the elimination of water and other volatiles (HCl vapors). The weight loss occurring between 200 and 400°C (60 wt %) is approximately the weight fraction of dopant. Above 400°C, the polymer itself decomposes. The TGA thermogram of PANI/D_{230}-MMT nanocomposite ($I_{c,d}$) containing 25, 50 wt % D_{230}-MMT and PANI/organoclay nanocomposites (II_b, III_b, IV_b) [Fig.7(b)] confirms the thermal stability. There is no sharp weight loss between 380 and 400°C as observed in PANI. This behavior is expected because the clay platelets protect and delay the intercalated chains from undergoing a degradation process. As the amount of D_{230}-MMT increased, the total weight loss of the nanocomposite decreased. It is suggested that, for the nanocomposites, the silicate layers (nanolayers) with a high aspect ratio (100–1000) are believed to effectively act as barriers, blocking the degradation of PANI chains located between the interlayer spacings. It was reported that the PANI chains for the intercalated nanocomposites are found to be more thermally stable than those for a simple PANI/MMT mixture containing the same amount of PANI (74.7 wt %).[39] This enhanced thermal stability in the nanocomposites was believed to be ascribed to the MMT nanolayers acting as barriers for the degradation of PANI in the interlayer spacings and partially related to the hindered diffusion of a volatile decomposition product within the nanocomposites and the shielding effect induced by the existence of the silicate nanolayers became more dominant with the increase of MMT content in the nanocomposites. In addition, the effect of clay concentration on the thermal stability of polypropylene (PP)/clay nanocomposite was studied. The thermal decomposition temperature of the nanocomposite was shifted to higher temperatures with increasing clay content. The temperature of the derivative weight loss of PP/clay (10.4%) was higher than that of pure PP by 44°C.[40]

CONCLUSIONS

A series of PANI/organoclay nanocomposites have been prepared by the intercalation of aniline monomer into interlayer spacings of MMT modified by different molecular weight of polyoxyalkylene followed by *in situ* oxidative polymerization of aniline monomers. It is evident from IR spectra that there are electrostatic interactions between the PANI chains and the MMT layers. It is observed from XRD studies that the peak characteristic to d_{001} was disappeared in PANI/organoclay nanocomposites at certain types and contents of organoclay. SEM and TEM observations suggest that PANI mineral lamellae are assembled to form nanodomains, whose average size was 150 and 250 nm depending on the organoclay content. Based on the TGA analysis, the PANI chains in the PANI/organoclay nanocomposites are more thermally stable than those of pure PANI. The room temperature conductivity varies

from 5×10^{-6} to 3.72×10^{-2} S/cm depending on the amount of PANI in the nanocomposites.

References

1. MacDiarmid, A. G.; Mu, S. L.; Somasiri, N. L. D.; Wu, W. Mol Cryst Liq Cryst 1985, 121, 187.
2. Novak, P.; Muller, K.; Santhanam, K. S. V.; Hass, O. Chem Rev 1997, 97, 207.
3. Kobayashi, T.; Yonevama, N.; Tamura, H. J Electroanal Chem 1984, 177, 281.
4. Batich, C. D.; Laitinen, H. A.; Zhou, H. C. J Electrochem Soc 1990, 137, 883.
5. Trinidal, F.; Montemayor, M. C.; Falas, E. J Electrochem Soc 1991, 138, 3186.
6. Dong, Y. H.; Mu, S. L. Electrochim Acta 1991, 36, 2015.
7. Hu, H.; Saniger, J. M.; Banuelos, J. G. Thin Solid Films 1999, 347, 41.
8. Cao, Y.; Paul, S.; Heeger, A. J. Synth Met 1992, 48, 91.
9. Heeger, A. J. Trends Polym Sci 1995, 3, 39.
10. Pud, A.; Ogurtsov, N.; Korzhenko A.; Shapoval, G. Prog Polym Sci 2003, 28, 1701.
11. Tsotra, P.; Gryschuk, O.; Friedrich, K. Macromol Chem Phys 2005, 206, 787.
12. Patel, H.; Somani, R. S.; Bajaj, H. C.; Jasra, R. V. Bull Mater Sci 2006, 29, 133.
13. Pinnavaia, T. J.; Beall, G. W. Polymer–Clay Nanocomposites; Wiley: New York, 2000.
14. Moet, A.; Akelah, A.; Hiltner, A.; Baer, E. Mater Res Soc Symp Proc 1994, 351, 91.
15. Salahuddin, N.; Shehata, M. Polymer 2001, 42, 8370.
16. Akelah, A.; Salahuddin, N.; Hiltner, A.; Baer, E.; Moet, A. Nanostruct Mater 1994, 4, 965.
17. Akelah, A.; Salahuddin, N.; Hiltner, A.; Baer, E.; Moet, A. Mater Lett 1995, 22, 97.
18. Salahuddin, N.; Moet, A.; Hiltner, A.; Baer, E. Eur Polym J 2002, 38, 1477.
19. Salahuddin, N. Polym Adv Technol 2004, 15, 251.
20. Salahuddin, N.; Rehab, A. Polym Int 2003, 52, 241.
21. Usuki, A.; Kojimai, Y.; Kawasumi, M.; Okada, A.; Fukushima, Y.; Kurauchi, T.; Kamigaito, O. J Mater Res 1993, 8, 1179.
22. do Nascimento, G. M.; Constantino, V. R. L.; Landers, R.; Temperini, M. L. A. Macromolecules 2004, 37, 9385.
23. do Nascimento, G. M.; Constantino, V. R. L.; Temperini, M. L. A. Macromolecules 2002, 35, 7535.
24. Bae, W. J.; Kim, K. H.; Jo, W. H. Macromolecules 2004, 37, 9850.
25. Lee, D.; Char, K.; Lee, S. W.; Park, Y. W. J Mater Chem 2003, 13, 2942.
26. Lu, J.; Zhao, X. Int J Modern Phys B 2002, 16, 2521.
27. Moreale, A.; Closs, P.; Badot, C. Clay Miner 1985, 20, 29.
28. Chang, T.-C.; Ho, S.-Y.; Chao, K.-J. J Chin Chem Soc 1992, 39, 209.
29. Carrado, K. A.; Xu, L. Chem Mater 1998, 10, 1440.
30. Kim, B. H.; Jung, J. H.; Hong, S. H.; Kim, J. W.; Choi, H. J.; Joo, J. Current Appl Phys 2001, 1, 112.
31. Colthup, N. B.; Daly, L. H.; Wiberley, S. E. Introduction to Infrared and Raman Spectroscopy, 3rd ed.; Academic Press: San Diego, CA, 1990.
32. Silverstein, R. M.; Bassler, G. C.; Morrill, T. C. Spectrometric Identification of Organic Compounds; Wiley: New York, 1967.
33. do Nascimento, G. M.; Contantino, V. R. L.; Landers, R.; Temperini, M. L. A. Macromolecules 2004, 37, 9373.
34. Kornmann, X.; Lindberg, H.; Berglund, L. A. Polymer 2001, 42, 4493.
35. Wu, Q.; Xue, Z.; Qi, Z.; Wang, F. Polymer 2000, 41, 2029.
36. Porter, T. L.; Thompson, D.; Bradley, M.; Eastman, M. P.; Hagerman, M. E.; Attuso, J. L.; Votava, A. E.; Bain, E. D. J Vac Sci Technol A 1997, 15, 500.
37. Kelly, P.; Akelah, A.; Qutubuddin, S.; Moet, A. J Mater Sci 1994, 29, 2274.
38. Mehrota, V.; Giannelis, E. P. Solid State Commun 1991, 77, 155.
39. Dongkyu, L.; Char, K. Polym Degrad Stab 2002, 75, 555.
40. Ma, J.; Qi, Z.; Hu, Y. J Appl Polym Sci 2001, 82, 3611.